

Evaluating the tracking effect on the performance of a hybrid photovoltaic system operating in a closed cooling cycle

Arkan Eltaief Khalaf^{1,*}, Muhammad Asmail Eleiwi¹, Tadahmun A. Yassen¹

¹ Mech. Eng. Dept., College of Eng., Tikrit University, Tikrit, Iraq.

arkan.a.khalaf43290@st.tu.edu.iq, muham76@tu.edu.iq, tadahmunahmed@tu.edu.iq

Abstract

In this paper, the electrical and thermal performance of a hybrid photovoltaic thermal system (PVT) operating with active cooling for a closed water cycle has been evaluated. Experimental tests were conducted on the hybrid photovoltaic thermal collector (PVT) to extract the heat from it for water heating purposes and reference photovoltaic collector (PV) in Iraq - Samarra, situated at the latitude (34.26° N) and the longitude (43.89° E). Several experimentations have been conducted through the months of March and May 2021 at main mass flow rates (m°_{wtr}) of (0.014 Kg/s), with different thermal loads ($m^{\circ}_{th,L}$) of (0.0031, 0.0046, and 0.0084 kg/s), and depending upon environmental circumstances. The results manifested that the maximum daily electrical ($\eta_{el_{PVT}}$), thermal (η_{th}), and the overall efficiency of PVT system ($\eta_{s,overall}$) with tracking was 9.7%, 34.4%, 44.1%, respectively at $m^{\circ}_{th,L}$ (0.0084 kg/s), and 9.28%, 27.8%, 37%, respectively without tracking at the same $m^{\circ}_{th,L}$. The highest improvement in the electrical power (E.P) of the PVT was 81.7% at $m^{\circ}_{th,L}$ (0.0084 kg/s) with tracking. Moreover, the present study evinced that the daily overall efficiency of the PVT collector ($\eta_{c,overall}$) and $\eta_{s,overall}$ were higher than those obtained by previous studies.

Keywords: PVT, Tracking, Cooling, Water jet

1. Introduction

The photovoltaic systems are the solution to the problem of carbon emissions and non-fossil fuels used to generate electricity. Solar cells that absorb sunlight and convert it into E.P can provide E.P supply in various fields. The photovoltaic system has advantages that other sources do not have. It is a medium power source and has a lengthy lifetime ranging within (20-30 years), also the operation of the system does not require a continuous human monitoring and many labors, its maintenance is low, and its components are easy to install [1] [2]. **Shihabudheen and Arun, 2014** [3] presented an analytical study of the PVT for water heating installed at Calicut-India (11° 15' N, 75° 46' E). The system consists of a mono PV panel with an area of 2.1 m², an absorption plate and copper tubes for transporting the cooling fluid, a tank with 100 L capacity, a water mass flow rate of 0.01 kg/s, and a glass cover placed over the PV panel to increase the thermal performance. It was found that the $\eta_{el_{PVT}}$, and η_{d-th} reached 10.5% and

30%, respectively. **Bahaidarah and Haitham, 2016** [4] introduced an experimental and numerical study to evaluate the performance for two systems; the uncooled (PV) system, and the cooled (PV) system by the water jet-impact cooling of the (PV) panels exposed to the climatic circumstances of the Dhahran city in the Middle East. Results showed that the temperature measurements for the solar cell were (69.7°C) and (47.6°C) for an uncooled system for June and December, correspondingly. After implementing a jet cooling, the average cell temperature decreased to (36.6°C) for June and (31.1°C) for December. The conversion efficiency and the power output were improved by (66.6%) and (51.6%) by applying a jet cooling for June, correspondingly. In December, the results elucidated an improved performance of (82.6%) in conversion efficiency and (49.6%) in power production. **Mustafa et al., 2018** [5] presented an experimental project of design and application of a simple as well as low-priced solar tracker system in Iraq - Baghdad with biaxial (azimuth angle and altitude angle) by utilizing Light Dependent Resistor (LDR). This project consists of a solar panel, LDR sensor module, dual-motor satellite dish, ball-joint, and an electronic circuit to obtain the maximum power from the solar panel. It was concluded that the maximum extraction of the energy from the sun was achieved by making the solar collector normal to the solar radiation, and the outcomes evinced that the solar tracker has more output power than the fixed solar panel by 35%. **Motahhir et al., 2018** [6] introduced an experimental study that includes a designed and implemented dual-axis active solar tracker (DAST) that tracks the sun using inexpensive components. A two-axis mechanism has been developed for controlling the (PV) panel tilt towards the higher concentration of the sunlight that captured via the (LDR) sensors, which being located at the (4) corners of (PV) panel. The model of the dual-axis active solar tracker has been built virtually as well as examined employing Excel to determine its efficiency. This study was conducted in Morocco, and the comparison based on the experimental results elucidated that the model of the dual-axis active solar tracker produced (36.26%) further power than the fixed panel. **Hasan et al., 2018** [7] presented an experimental and theoretical study that included the design and implementation of a PVT with a system of water jet collision. The indoor testing system was conducted by using the solar simulator in the laboratory. The levels of solar radiation were varied from (500 W/m²) to (1000 W/m²) in the indoor test. At each solar radiation, the level of water (m°_{wt}) was changed from (0.033 kg/s) to (0.16 kg/s). The experimental results showed when applying water jet cooling, the maximum PV, thermal, and total PVT efficiencies were 11.35%, 72%, and 81%, respectively at the solar radiation intensity level of 1000 W/m². The mathematical results were close to the experimental results with an accuracy of (95.8%) and (99.6%) for the (PV) and the thermal (PVT) efficacy, correspondingly. **Kim et al., 2019** [8] conducted an experimental and numerical work of the use of passive cooling technology for photovoltaic panels using heat sinks. The experimental work was conducted in Korea, the meshes made of aluminum and iron being used as one of the passive cooling techniques, and the indoor tests were conducted using a solar simulator to analyze the performance of cooling. In the experimental work, it was found that the temperature of aluminum and iron meshes reduced the temperature of the PV module by 6.56°C and 4.35°C, correspondingly. The numerical results showed that the cooling performance is better when using the fins compared to the metal meshes. **Barone et al., 2019** [9] presented an inventive water PVT prototype. The collector consisted of a poly-crystalline photovoltaic module and installed on its back eleven plastic pipes inside an aluminum box for heating the water. Practically, the PVT was connected to a thermosiphon storage tank. The tests were conducted experimentally at the Patras University (in Greece). The prototype can provide both electricity and hot water for the domestic use. An appropriate model of the dynamic simulation was evolved and confirmed versus the investigational data. This system operates at (2) various rates of flow (0.013) kg/sec and (0.016) kg/sec and at a tilt angle (30° and 50°). Experimental results showed that the maximum thermal and electrical efficiency of the PVT system was 25% and 16%, respectively, and a very good agreement was between the

experimental and the simulated values. **Vladimir Ivanovich et al., 2010** [10] introduced an experimental work that combines both the active and passive cooling techniques for improving the electrical output of a (PV) module. An ultrasonic humidifier and the fins made up of aluminum as a heat sink was used to cool the PV panel. The purpose of using an ultrasonic humidifier is to generate a humid environment at the backside of the PV panel. The cooling system was capable to decrease the (PV) average temperature via (14.61°C), and such decrease achieved a (6.8%) enhancement in the efficacy of PV. The average power of the cooled panel reached (12.23 W) against (10.87 W) for the uncooled panel. The total consumption of water reached approximately 1.5 L through the entire investigational procedure owing to the evaporation.

All previous studies did not use a jet collision water technology at outdoor testing for cooling the (PV) panel and for heating the water with the use of a solar tracking system under the Iraqi weather conditions. The present study used jet collision water cooling with tracking by the outdoor testing under the climatic Iraqi conditions to better evaluate the tests of PVT and PV. The aim of the present work is to conduct a practical study to know the effect of m°_{wtr} , $m^{\circ}_{th,L}$, and tracking on the performance of the PVT and their role in heating the water to the best level for the domestic use. The work was performed under the environmental conditions of Samarra city in Iraq.

2. Methodology

Here, the assembly of system, the principle of operating, the setup of experiment, and the instrumentations are explained. This system consists of two photovoltaic collectors, one PV and the other a PVT collector for water heating, comprising a thermally insulated cold and hot water tank (HWT), and a thermally insulated rear cooling basin. The PVT collector is equipped with a manual mechanism that allows it to track the sun.

2.1. PVT System assembly

Monocrystalline solar cells having the dimensions (length 148 cm and width 68 cm) were used. The cooling basin is attached to the PV rear surface and it is made of galvanized iron with a thickness of (0.1 cm) in a form of a rectangular basin with dimensions (length 148 cm * width 68 cm * height 15 cm). Ten nozzles with (0.04 cm) diameter for each of them were installed on the basin back, distributed uniformly in two rows and (30 cm) away from the outer edges and from each other at regular distances in order to install the water jets that are connected to flexible tubes, as shown in the figure (1). This distance ensures that the water is evenly distributed over the entire back area of the PV panel when the water is pumped into the nozzles by the electric pump. To reduce the heat loss from the walls and pipes of the basin to the outer surrounding, the basin is insulated with glass wool available in the local markets, with a thickness of 5 cm and with thermal conductivity (0.045 W/m. $^{\circ}\text{C}$). The PVT is equipped with a manual mechanism to allow it to track the sun for making the solar radiation normal on panel surface through the day for increasing the intensity of solar radiation falling on the panel through the day, and this will lead to an increase in the electrical and thermal energy (Q_{th}) at the same time. The PVT and PV are equipped with a flexible bar to adjust the inclination angle of them from the horizon with the change of time during the year for the city of Samarra to make the solar radiation normal on the panels according[11]. The water tank is made of galvanized iron with a capacity of 20 L. The tank is insulated from the outside to reduce the heat losses and it is equipped with a float to control the amount of water entering it from the cold water tank (CWT) which feeds the HWT with cold water when there is $m^{\circ}_{th,L}$, as well as two valves installed at the bottom, one to control the amount of water flowing into the pump and the other to adjust the amount of $m^{\circ}_{th,L}$. Further explanations about the construction parameters are comprised in Table (1).

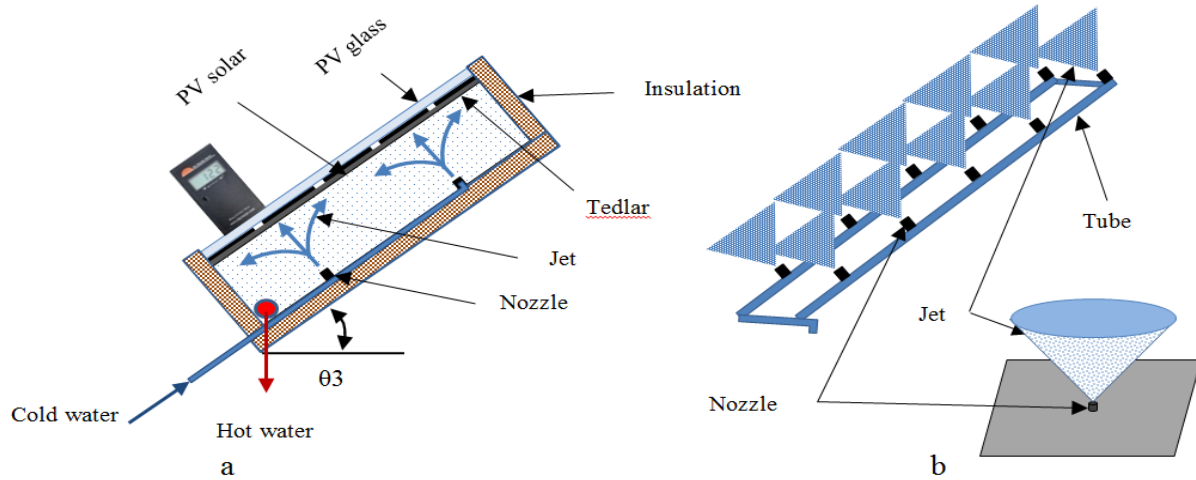


Figure (1): (a) Profile of the PVT, and (b) Nozzles Connecting

Table (1): PVT specifications

Part	Item	Technical Specifications
PV Panel	Cell Type	Monocrystalline
	Maximum Power (P max)	150 W
	length	148 cm
	Width	68 cm
	Thickness	4 cm
	Front cover	Tempered glass
Charger Controller	Absorbance	0.95
	Type	PWM
	Rated Current	30A
Battery	Rated Voltage	12v/24v
	Number	2
	Capacity	48 AH
Water Pump	Voltage	12 V
	Type	Diaphragm Pump
	Power/voltage	30watt/24 VDC
Step-up Boost Converter	Working flow	1.1 LPM
	Type	150 W DC-DC
	Input Voltage	10 v – 30 v DC
Rear cooling basin	Output Voltage	12v – 35v DC
	Material	Galvanized steel sheet
	length	148 cm
	Width	68 cm
	Height	15 cm
Insulation	Thickness	0. 1 cm
	Material	Glass wool

	Thickness	5 cm
	Thermal conductivity	0.045W/m. $^{\circ}$ C
Nozzle	Material	Metal
	Number	10
	Jetting hole diameter	0.04 cm
	Material	Galvanized steel sheet
HWT	Capacity	20L
	Thickness	0.1 cm

2.2. Experimental installation and instruments

Twelve k-type thermocouples were used to measure the temperature at specific locations of the PVT and PV, can measure the temperature in the range (0-200°C), and are installed as follow:

Three thermocouples are on the PVT surface, three on the PV surface, one at the water inlet to the PVT, one at the water outlet from the PVT, one inside the HWT, one at the drain of the HWT (for $m_{th,L}$), one from the CWT, and one to measure the ambient temperature. All these sensors are connected to a manual selector switch (SS) to select the thermocouple whose temperature is to be measured. The SS is connected in turn to a digital thermometer within the range (-50°C to 1300°C) to measure the temperature with an accuracy of 0.3% and to read the temperature of each thermocouple selectable from the SS. A solar meter (type Daystar.inc DS-05A) is used to measure the radiation intensity with an accuracy of 3%. A digital relative humidity meter (type LT-2) is utilized with an accuracy of 5%. The Avometer (type VC10C) with an accuracy of 0.8% is portable to measure the voltage of batteries. A volt and current meter (type Mini Panel meter dual LED Display) is employed with an accuracy of 1%. An electric diaphragm pump (type CSC-100) with a power of 30 watts is used to circulate water from the tank and to the collector with a power of 30 watts at a maximum water flow rate of 1.1 LPM. A flowmeter (type LZS-15 ½") is utilized with an accuracy of 4% for measuring the rate of pump water flow, such rate of flow can be governed by a valve, and the pump's E.P can be controlled through regulator voltages. A glass beaker is utilized for measuring and adjusting the volumetric flow rate of $m_{th,L}$. Figure (2) depicts the investigational work's setup.

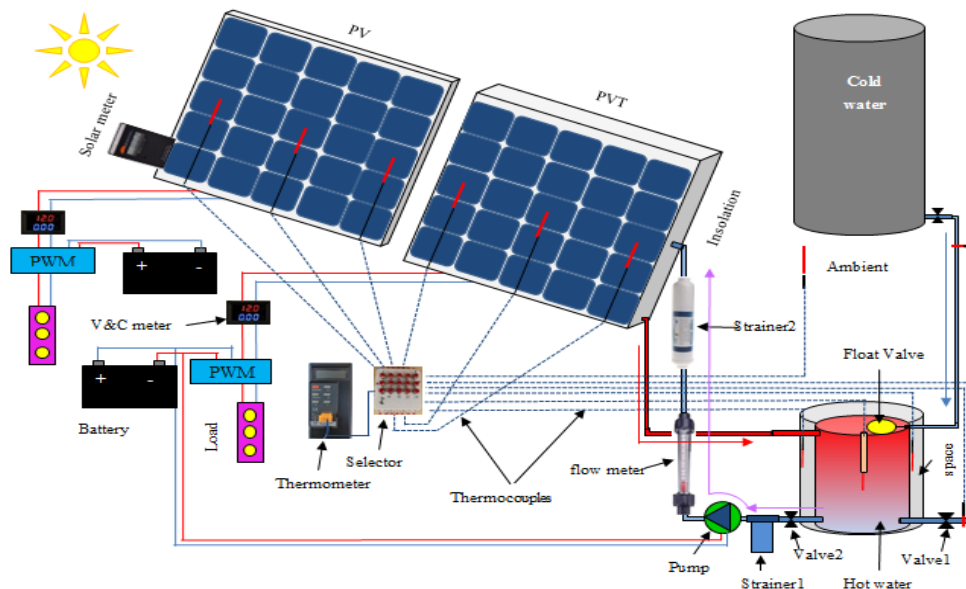


Figure (2): The schematic diagram of the PVT system

2.3. Experimental Work

Experiments being conducted outdoor in the northern suburb of Samarra-Iraq (latitude 34.26°N and longitude 43.89°E) for two cases (with and without tracking) and with the main m_{wtr}° of (0.014 kg/s) in each case. The $m_{\text{th},L}^{\circ}$ was taken with the test start-up at 8:30 am until the end at 4:30 pm with three values of $m_{\text{th},L}^{\circ}$ of ($0.0031, 0.0046, 0.0084 \text{ kg/s}$). The electrical load is (100 Watt) in each case. The experimental data were recorded from 8:30 am to 4:30 pm. The inclination angle of PVT and PV is adjusted from the horizon with the change of time during the year at the latitude angle (34.26°) for the city of Samarra to make the solar radiation normal on the panels. At the beginning of each experience, the sunny climate is selected free of clouds, and the PVT and PV are cleaned thoroughly, tracking the sun manually. The hot and cold water tanks are cleaned and filled with distilled water, fully pre-charged the batteries, connect the charge controller to PVT and PV, connect the pump to the battery, and the mass flow is adjusted through the flow meter. The measuring instruments are turned switched on. The data are recorded at the end of each (30 minute). The assembly of the PV and PVT parts prepared for testing is shown in figure (3). The study encompasses the following models:

- 1- PV without cooling and PVT using water as a cooling fluid without tracking.
- 2- PV without cooling and PVT using water as a cooling fluid with tracking.

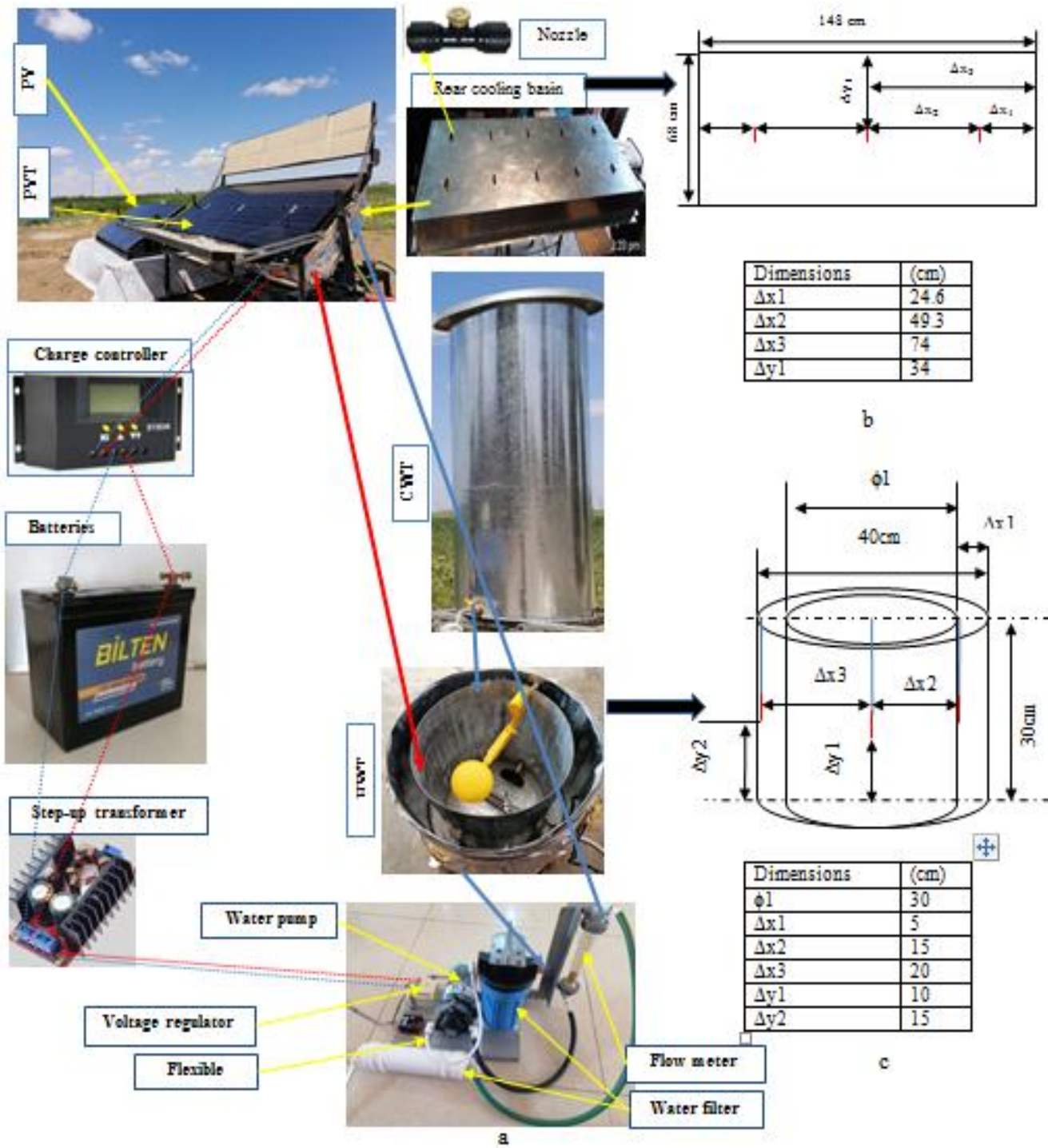


Figure (3): (a) Experimental PVT test rig, (b) Locations of the thermocouples on the PV panel, and (c) Thermocouples locations inside the HWT

2.4. Calculations

Table (2): Mathematical formulas calculations

The heat input to the PV and PVT is[12] [13]: $Q_{in} = \int_0^t I_T A_{PV} dt \quad (1)$
The energy saved in the tank is [14]: $Q_{stor} = M_{wtr} Cp_{wtr} (T_{wf} - T_{wi}) \quad (2)$
The daily useful thermal energy from the PVT is [15]: $Qu = m^{\circ}_{wtr} Cp_{wtr} \int_0^{t1} (T_{colle.out} - T_{colle.in}) dt \quad (3)$
The total $m^{\circ}_{th,L}$ energy taken from the water tank is [16] [17]: $Q_L = m^{\circ}_{th,L} Cp_{th,L} \int_0^{t1} (T_{th,L.out} - T_{c.w.in}) dt \quad (4)$
The average daily thermal efficiency with $m^{\circ}_{th,L}$ is [18]: $\eta_{d.th} = \frac{Q_{store} + Q_L}{Q_{in}} \quad (5)$
The average daily thermal efficiency of system is : $\eta_{d.th} = \frac{M_{wtr} Cp_{wtr} (T_{wf} - T_{wi}) + m^{\circ}_{th,L} Cp_{th,L} \int_0^{t1} (T_{th,L.out} - T_{c.w.in}) dt}{A_{PVT} \int_0^t I_T dt} \quad (6)$
The E.P generated from the solar cell is: $E.P_{PV} = I * V \quad (7)$
The daily electrical efficiency rate is [2] : $\eta_{el_{PV}} = \frac{\int_0^{t1} V_{PV} * I_{PV} dt}{A_{PV} \int_0^t I_T dt} \quad (8a)$
$\eta_{el_{PVT}} = \frac{\int_0^{t1} V_{PVT} * I_{PVT} dt}{A_{PVT} \int_0^t I_T dt} \quad (8b)$
The overall efficiency is: $\eta_{overall} = \eta_{PV} + \eta_{th} \quad (9)$

3. Experimental uncertainty analysis

The sources of errors are widely classified into (3) groups of error groups: Calibration, Data collection, and Data reduction. There're numerous error sources of the element for each group. The producer delivered the measuring devices or apparatuses and different information systems with a list of specifications, like The independent parameters, like temperature drifts, linearity, deceleration, repetition, accuracy, relative humidity, precision limit (P) solar radiation, and the bias error (B) employing the technique of Collect-Root-Sum Squares (RSS)[19][20] , as in Table (3).

Table (3): Mathematical formulas of uncertainty

The bias error (B) can calculate from:	$B = \pm \sqrt{(0.5 * Resolution)^2 + (Accuracy)^2}$ (10)
(\bar{X}) : The scale mean value or the measuring mean is:	
$(\bar{X}) = \frac{1}{n} \sum_{i=1}^n X_i$	(11)
The standard deviations (σ_x) of the sample distribution is:	
$\sigma_x = \frac{\sigma_x}{\sqrt{n}}$	(12)
The entire precision error limits are expressed as:	
$P_x = t(N - 1), 95\% * \sigma_x$	(13)
For obtaining a 95% confidence of uncertainty (U_x):	
$U_x = \pm [B^2 + P_x^2]^{1/2}$	(14)
The relative uncertainty (in percentage) is calculated as:	
$\frac{U_x}{X} \% = \pm \left(\frac{U_x}{X} \right) * 100$	(15)

The uncertainty calculation for the mentioned parameters in the present paragraph is depicted in the Table (4).

Table (4): The uncertainty of the measured parameters

	B	X̄	σx	σ̄x	Px	Ux	Ux / X %
I (W/m ²)	± 0.5	990.49	45.24	22.6	71.913	71.914	±7.26
Ø %	±0.07	38	2.58	1.29	4.104	4.105	±10.8
T _{amb} (°C)	±0.05	25.02	0.93	0.46	1.463	1.464	±5.85
T _{in} (°C)	±0.05	33.58	1.12	0.56	1.781	1.782	±5.3
T _{out} (°C)	±0.05	42.85	1.26	0.63	2.004	2.005	±4.67
T _{tank} (°C)	±0.05	36.02	1.26	0.63	2.004	2.005	±5.56
T _{L out} (°C)	±0.05	35.04	1.26	0.63	2.004	2.005	±5.72
T _{L in} (°C)	±0.05	27.27	0.99	0.49	1.559	1.559	±5.72
T _{PVT} (°C)	±0.05	47.65	1.22	0.61	1.941	1.941	±4.07
T _{PV} (°C)	±0.05	53.67	1.53	0.76	2.418	2.418	±4.5
I (Amp)	±0.01	4.97	0.08	0.04	0.127	0.127	±2.56
V (Volt)	±0.05	16.77	0.26	0.13	0.413	0.416	±2.48

4. Results and Discussion

In this section, the experimental study of the overall system performance upon the ecological circumstances (sunny day) of the Samarra city in Iraq has been introduced. Many experiments were conducted through (March, May 2021). The PVT has been tested with and without tracking. For the PV and PVT, one can compute the $\eta_{el.PV}$ and $\eta_{el.PVT}$ from the equations (8a) and (8b), respectively. For the

PVT, one can compute the η_{d-th} from equation (6). The ($\eta_{s,overall}$) of PVT can be calculated from the equation (9).

4.1. PVT with $m^{\circ}_{th,L}$ and without tracking

For studying the overall system performance of the PVT, the system was tested without tracking. The test was conducted on (29/3/2021, 28/3/2021, and 26/3/2021) with $m^{\circ}_{th,L}$ of (0.0031, 0.0046, and 0.0063 kg/s), correspondingly at the main cooling water flow rate of (0.014 kg/s). Figures (4a-4c) evince that the solar radiation first starts to rise from the first hour of the test (8:30 am) and reaches its highest value (1154.7, 1140, and 1047.1 W/m²) at 12:30 pm on 29/3/2021, 28/3/2021, and 26/3/2021, respectively and then begins to decrease gradually. It was noted in the same figures that the relative humidity changes with the hours of the day, which is inversely proportional to the intensity of solar radiation.

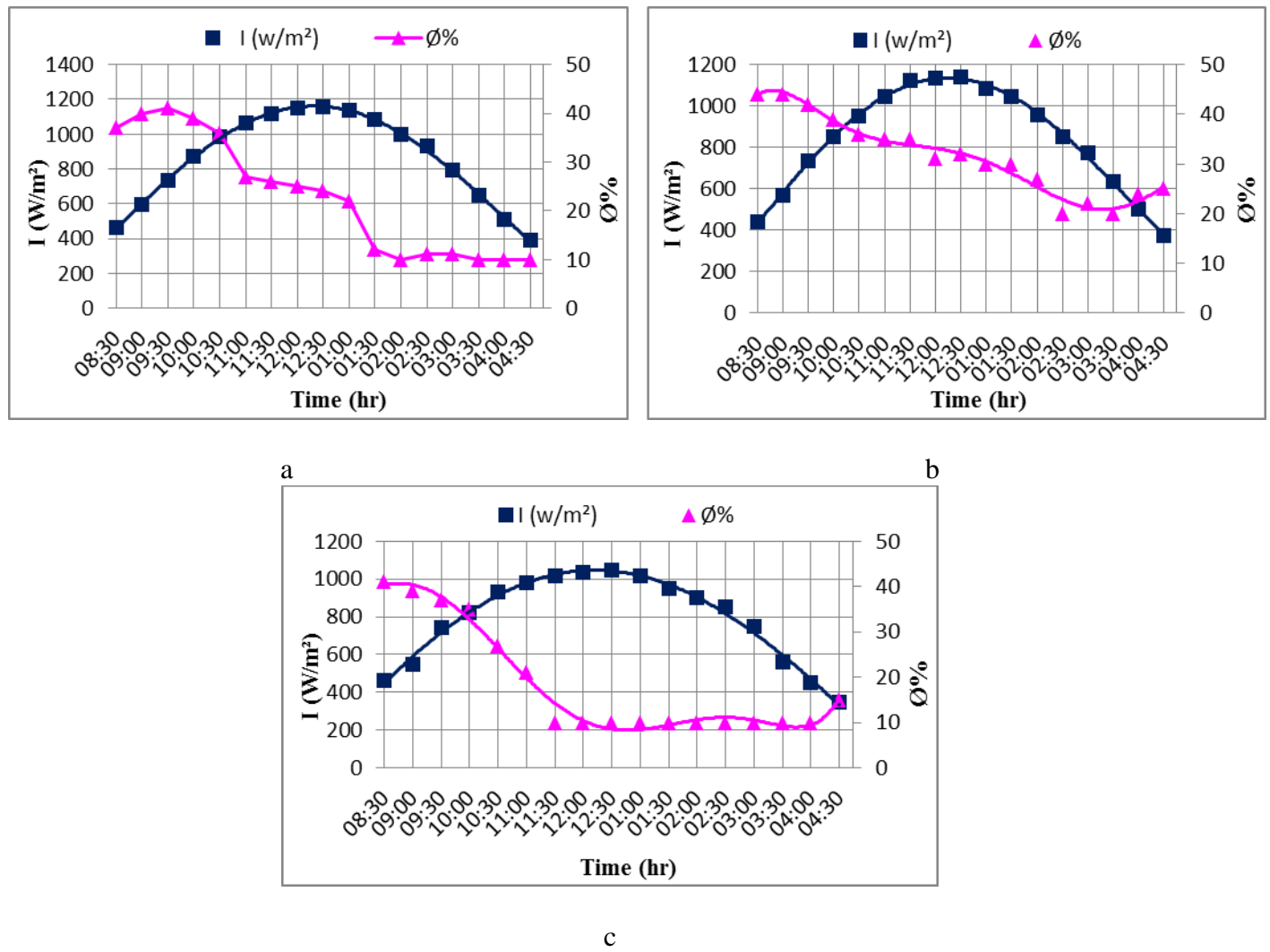
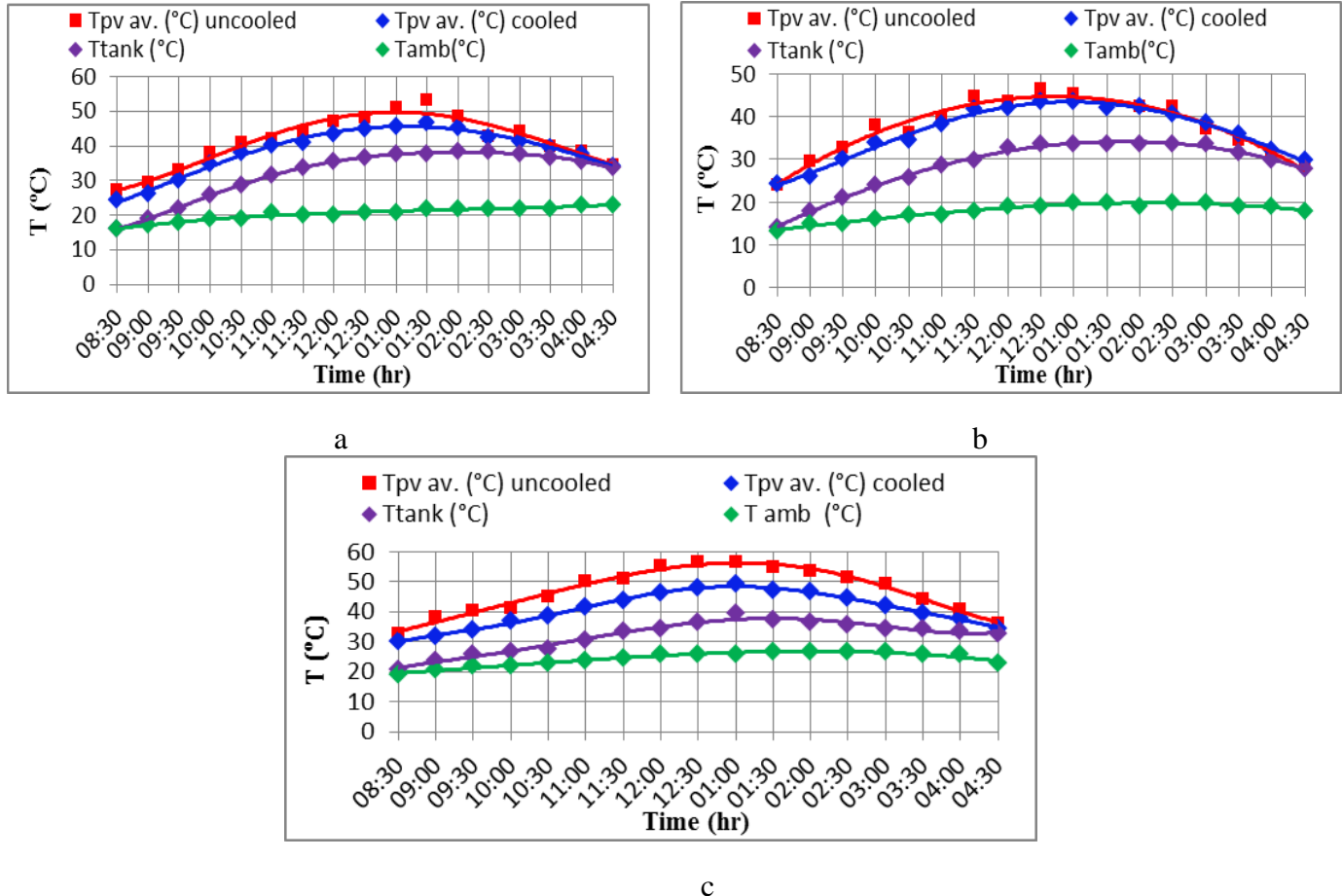


Figure (4): The change in the solar radiation intensity and humidity with the time on:
 (a) 29/3/2021, (b) 28/3/2021, and (c) 26/3/2021

Figures (5a-5c) manifest the change of the temperature of the PVT and PV, tank water temperature, and ambient temperature with the local time. The maximum value of the PVT and PV surface temperature

was first (46, 53°C) on 29/3/2021 at 1:30 pm, (43, 46°C) on 28/3/2021 at 12:30 pm, and (48, 57°C) on 26/3/2021 at 1:00 pm with $m_{th,L}$ of (0.0031, 0.0046, and 0.0063 kg/s), respectively and then decreased with the decreasing of the solar radiation intensity. The maximum value of HWT was 38°C, 33.5 °C, and 39°C on 29/3/2021, 28/3/2021, and 26/3/2021, respectively. Figure (5c) shows the temperatures difference between the PVT and PV surfaces . It was observed that this difference was the largest compared to other figures due to the presence of the high $m_{th,L}$ on the HWT.



Figures (5): The change of temperatures with time with $m_{th,L}$ of (0.0031, 0.0046 and 0.0063 kg/s) on:
(a) 29/3/2021, (b) 28/3/2021, and (c) 26/3/2021, respectively

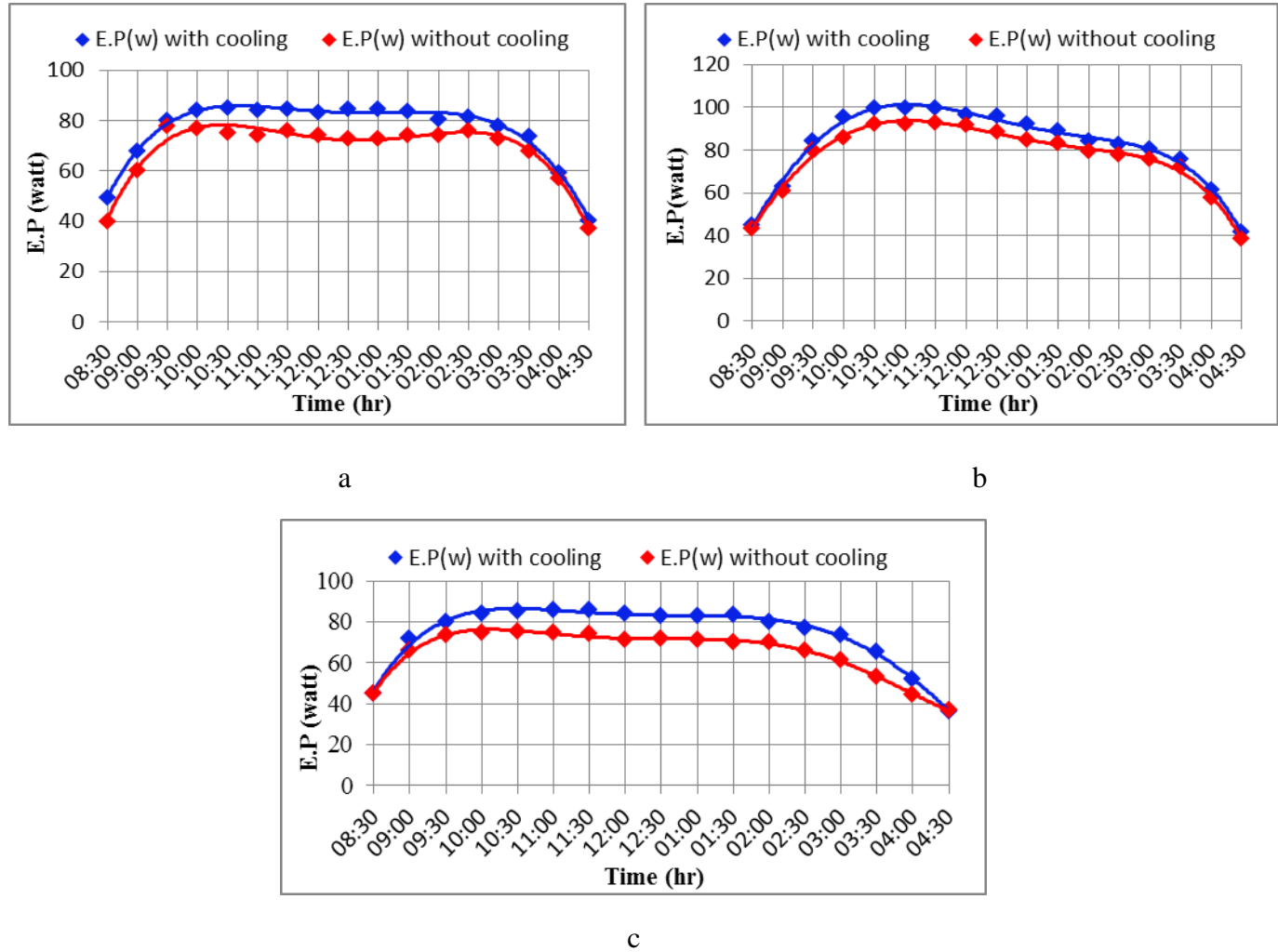
Figures (6a-6c) reveal the change in E.P produced from the PVT and PV with the local time. From these figures below, one can notice that the E.P produced began to rise since the early morning hours. The maximum value of the PVT and the corresponding value for PV was (85, 75 W) on 29/3/2021 at 10:30 am, (99.6, 92.6 W) on 28/3/2021 at 11:30 am, and (86, 75 W) on 26/3/2021 at 11:00 am with $m_{th,L}$ of (0.0031, 0.0046, and 0.0063 kg/s), respectively. It was observed that the electrical generation first decreased due to the increase of PV and PVT temperature at 12:00 pm, 12:30 pm, and 12:00 pm for the figures (6a to 6c), respectively and then decreased gradually with decreasing the intensity of solar radiation. For all these three figures, the PVT remained superior to the PV in electrical production from 8:30 am until the last reading at 4:30 pm due to the use of $m_{th,L}$.

At the 1st $m_{th,L}$ (0.0031 Kg/s), the total electrical energy (Q_{el}) produced from the PVT and PV was (2.23, 2.01 MJ), respectively with an enhancement of 10.9%, at the 2nd $m_{th,L}$ (0.0046 Kg/s), it was (2.41, 2.25 MJ), respectively with an enhancement of 7.1%, and at the 3rd $m_{th,L}$ (0.0063 Kg/s), it was (2.18, 1.9 MJ).

Copyrights @Kalahari Journals

Vol. 7 No. 1(January, 2022)

MJ), respectively with an enhancement of 14.7%. The highest percentage of enhancement in the electrical performance of the PVT was 14.7% at the 3rd $m^{\circ}_{th,L}$, and the reason is that the greater the $m^{\circ}_{th,L}$ extracted from the HWT, the greater the heat extraction from the PVT, which leads to a decrease in its temperature and then an increase in its E.P. It was noted from these three cases that the best cooling was at the 3rd $m^{\circ}_{th,L}$.

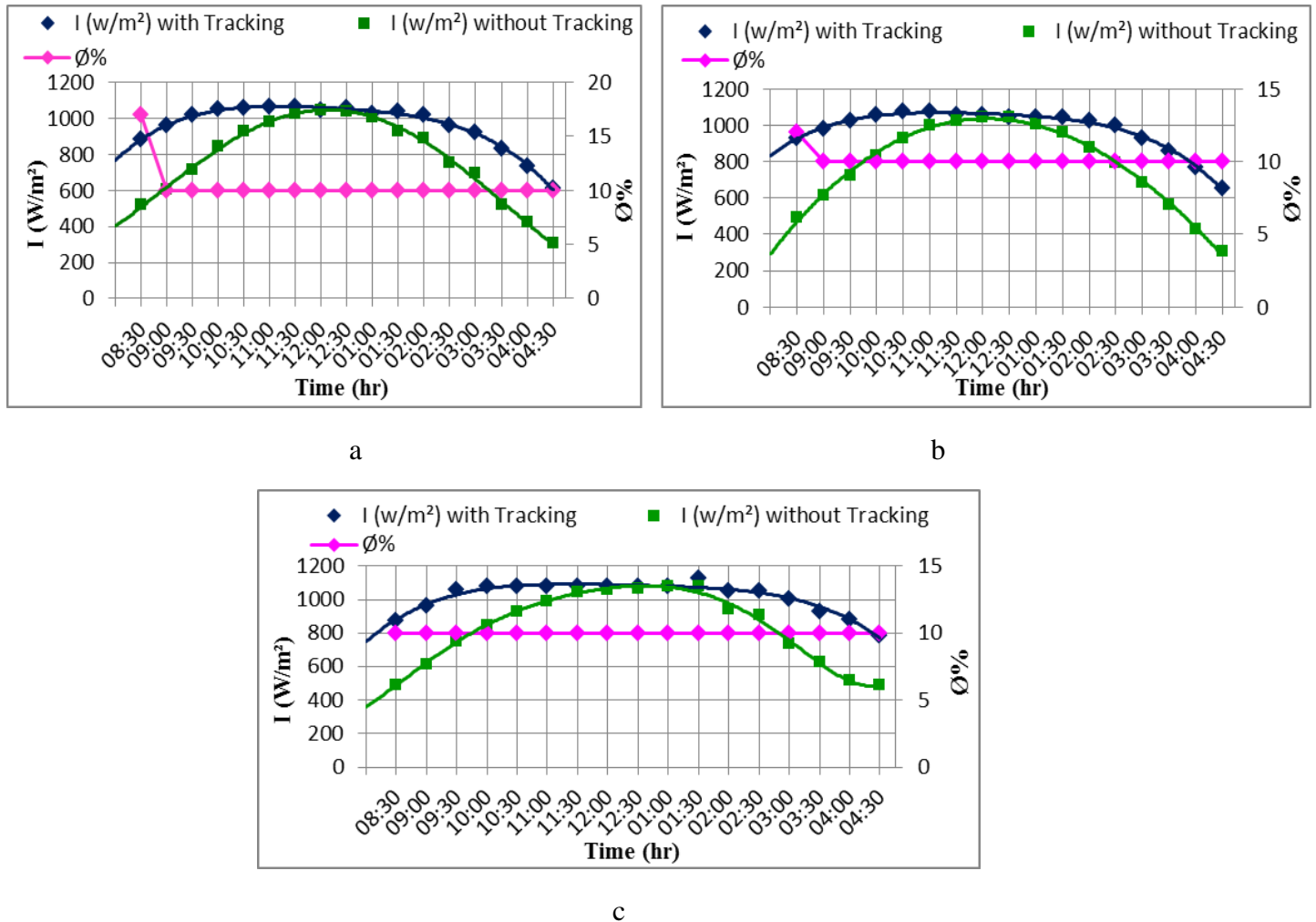


Figures (6): The change in the E.P produced from PVT with using $m^{\circ}_{th,L}$ of (0.0031, 0.0046, and 0.0063 kg/s) and PV with time on: (a) 29/3/2021, (b) 28/3/2021, and (c) 26/3/2021, respectively

4.2. PVT with $m^{\circ}_{th,L}$ and with tracking

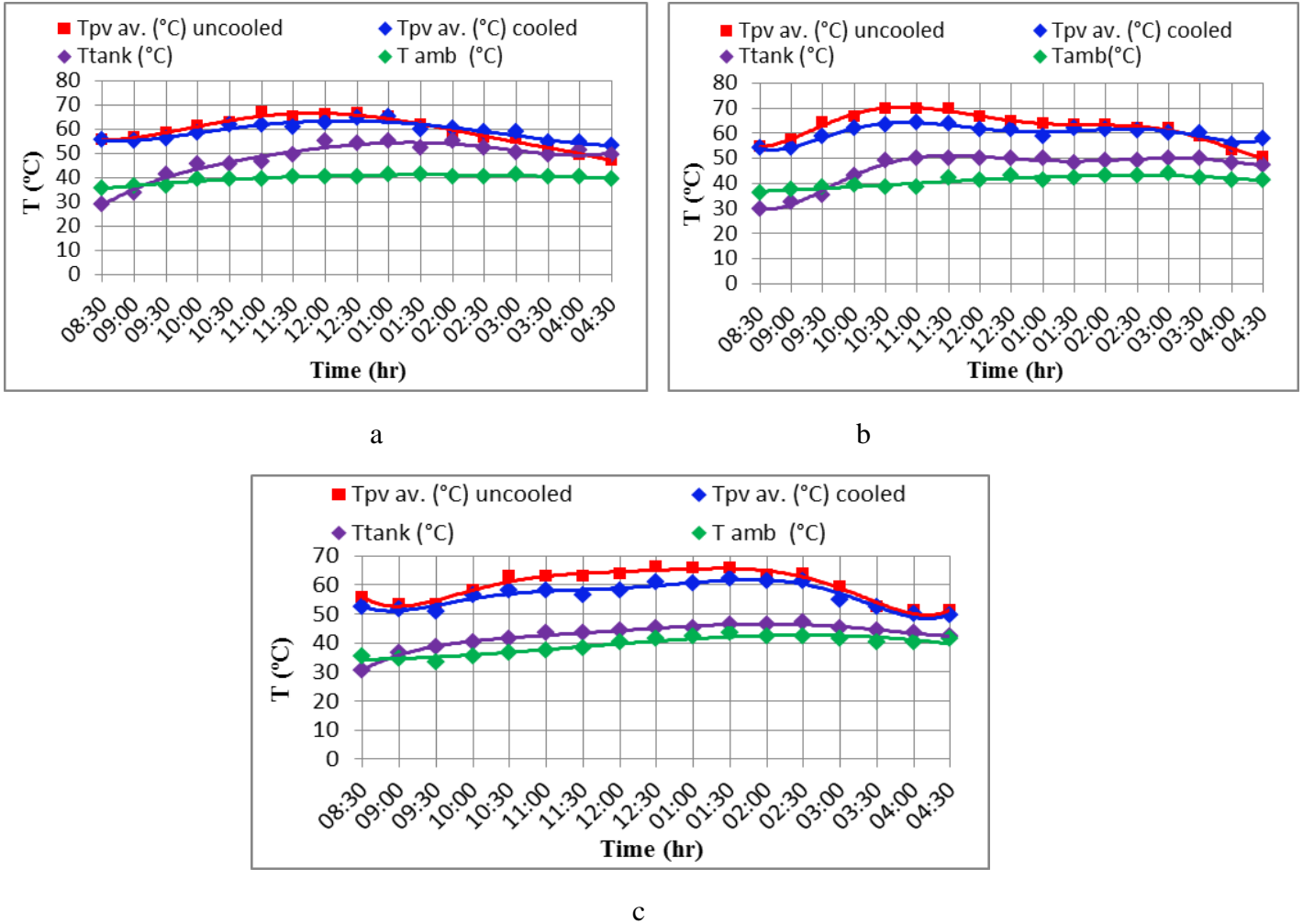
For studying the overall performance of the photovoltaic system, the PVT system was tested with tracking and PV without tracking. The test was conducted on (15/5/2021, 16/5/2021, and 17/5/2021) with $m^{\circ}_{th,L}$ of (0.0031, 0.0046, and 0.0084 kg/s), correspondingly at the main cooling water flow of 0.014 kg/s. Figures (7a-7c) depict the solar radiation change for PVT and PV, as well as the relative humidity with the local time. The ultimate solar radiation determined through the PVT experiment with the corresponding value of PV was (1066.6, 978.6 W/m²), respectively on 15/5/2021 at 11:00 am, (1076.4, 998.2 W/m²), respectively on 16/5/2021 at 11:00 pm, and (1125.3, 1076.4 W/m²), respectively on 17/5/2021 at 1:30 pm. The daily solar radiation for PVT and PV was (28, 23 MJ/ m²) for figure (7a),

(28.5, 23.27 MJ/m²) for figure (7b), and (29.58, 24.63 MJ/m²) for figure (7c) with a percentage increase of 21.7%, 22.4%, and 20%, respectively, due to the presence of the tracking, which increases the intensity of the solar radiation falling on the PVT. It was noted in the same figures that the relative humidity was stable at 10% during the daylight hours.



Figures (7): The change of the solar radiation intensity and humidity with the time on: (a)15/5/2021, (b)16/5/2021, and (c)17/5/2021, respectively

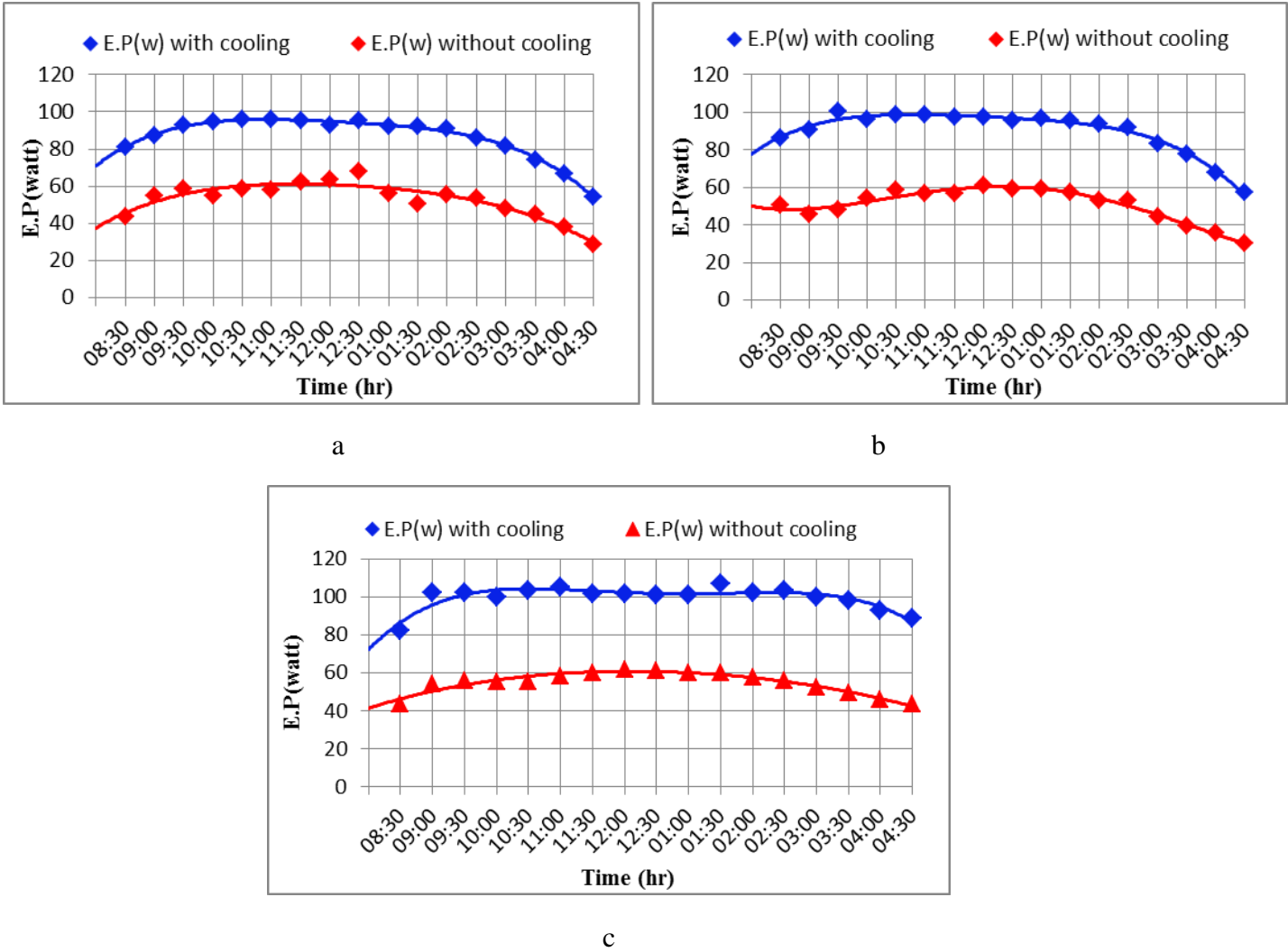
Figures (8a-8c) view the variation of the PVT and PV temperatures, maximum tank water temperature, and ambient temperature with the local time. The maximum temperature value of the PVT with the corresponding value of PV was first (65°C) for each on 15/5/2021 at 1:00 pm, (64, 70°C) on 16/5/2021 at 11:00 pm, and (62, 65.8) on 17/5/2021 at 1:30 pm with $m_{th,L}$ of (0.0031, 0.0046, and 0.0084 kg/s), respectively, and then decreased with the decreasing of the solar radiation intensity. The maximum value of HWT was 55°C, 50°C, and 47°C, on 15/5/2021, 16/5/2021, and 17/5/2021, respectively. Figure (8c) shows that the PVT temperature was less than the PV temperature from 8:30 am until the end of the test at 4:30 pm despite the presence of the tracking that causes an increase in the solar radiation intensity. This is due to the presence of the biggest $m_{th,L}$ (0.0084kg/s) on the HWT which led to the large temperature difference between PVT and PV compared to the other cases.



Figures (8): The change of temperature with the time in the presence of both tracking and $m^{\circ}_{th,L}$ of (0.0031, 0.0046, and 0.0084 kg/s) on: (a) 15/5/2021, (b) 16/5/2021, and (c) 17/5/2021, respectively

Figures (9a-9c) portray the change in the E.P produced from the PVT (in the presence of $m^{\circ}_{th,L}$ with tracking) and the PV with the local time. It was noticed that the E.P produced from the PVT and PV began to rise since the beginning of the test at 8:30 am. The maximum power value for the PVT and the corresponding value for PV was first (96, 58.5 W) on 15/5/2021 at 10:30 am, (100.6, 47.8W) on 16/5/2021 at 9:30 am, and (106.6, 60W) on 17/5/2021 at 1:30 pm with $m^{\circ}_{th,L}$ of (0.0031, 0.0046, and 0.0063 kg/s), respectively and then decreased gradually with the decreasing of the intensity of solar radiation with the large difference between PVT and PV as a result of tracking, and the PVT remained the highest production of E.P from the 8:30 am until the end of the test at 4:30 pm.

The Q_{el} produced from the PVT and PV was (2.52, 1.54 MJ), (2.61, 1.48 MJ), and (2.89, 1.59MJ) with an enhancement of 63.6%, 76.3%, and 81.7% with $m^{\circ}_{th,L}$ of (0.0031, 0.0046, and 0.0084 kg/s), respectively. It was observed that the highest enhancement rate was 81.7% due to the presence of the tracking that increased the intensity of solar radiation with using the biggest $m^{\circ}_{th,L}$ (0.0084 kg/s) drawn from the HWT, which extracted the heat from PVT and led to a decrease in the PVT temperature, therefore led to an increase in the E.P production.



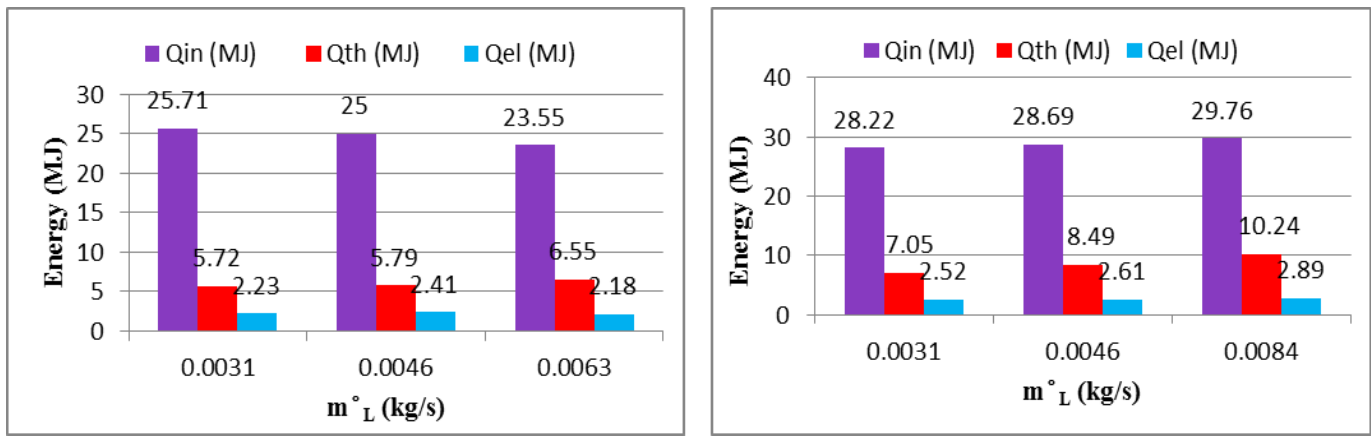
Figures (9): The change in E.P produced from PVT with using tracking and $m^{\circ}_{th,L}$ of (0.0031, 0.0046, and 0.0084 kg/s) and PV with the time on: (a) 15/5/2021, (b) 16/5/2021, and (c) 17/5/2021, respectively

4.3. The overall electrical and thermal efficiency of the PVT

Figures (10a-10b) illustrate the variation of energy balance for the total input energy and the total energy output (sum of electrical and thermal energy) for the PVT without and with tracking at three values of $m^{\circ}_{th,L}$, respectively. The energy quantity that received from the solar radiation (input energy) without tracking will be less than the energy received with tracking, so the output energy with the tracking will be higher than the output energy compared to without tracking. Figure (10a) shows that the maximum total energy output was (8.73 MJ) without tracking, at the 3rd $m^{\circ}_{th,L}$, while it was seen from the figure (10b) that the highest total energy output was (13.13 MJ) with tracking, at the 3rd $m^{\circ}_{th,L}$, which was greater than the total energy output at the 1st and 2nd $m^{\circ}_{th,L}$ with an enhancement of 37.2% and 18.2%, respectively.

Figure (11) presents the variation of the $\eta_{s,overall}$ for two models (without tracking, with tracking) with three values of $m^{\circ}_{th,L}$, respectively. It was observed that the $\eta_{s,overall}$ increased significantly with the increasing of the $m^{\circ}_{th,L}$ because of the reduction in the PVT temperature, and it was also noted that the $\eta_{s,overall}$ with using tracking is bigger than the $\eta_{s,overall}$ without using tracking, because the tracking increased the intensity of solar radiation. The maximum $\eta_{s,overall}$ was 44.13% and 37%, with and without

tracking, respectively. The highest $\eta_{s,overall}$ was reached 44.13% in the presence of tracking at the 3rd $m^{\circ}_{th,L}$.



(a) PVT without tracking

(b) PVT with tracking

Figure (10): The energy variation with the $m^{\circ}_{th,L}$ (kg/s)

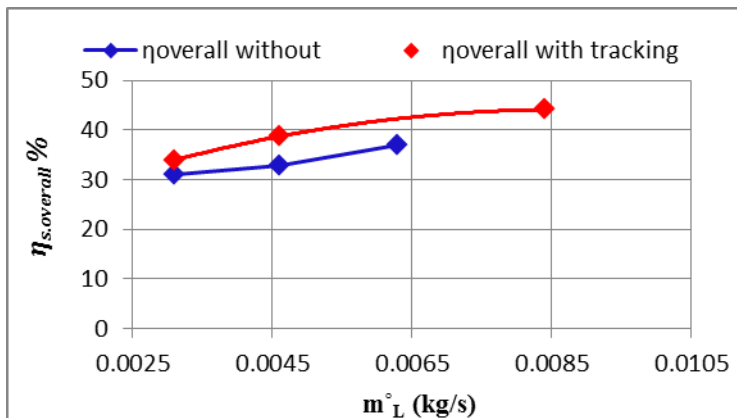


Figure (11): The $\eta_{s,overall}$ variation with the $m^{\circ}_{th,L}$ (kg/s)

4.4. Comparison of current study with preceding studies

A comparison of the results of the current study with the results of previous studies on the experimental and theoretical work is given in Table (8) indicating the as follows:

- 1- Compared to the previous work by Shihabudheen and Arun [3], who obtained the $\eta_{c,overall}$ reached 39.8% without tracking at m°_w (0.01 kg/s), the $\eta_{c,overall}$ in the current study was 48% without tracking at m°_w (0.014 kg/s) with $m^{\circ}_{th,L}$ (0.0084 kg/s), and the weather conditions were better than the weather conditions of the previous studies. The $\eta_{c,overall}$ of the current study is superior to the $\eta_{c,overall}$ of the previous study despite using glass cover and PV above an absorber plate made of copper which has a high thermal conductivity.
- 2- The $\eta_{c,overall}$ in previous work by Barone et.al.[9] was 38.6% with tracking at m°_w (0.016 kg/s), whereas in the current work, it was 52% and 48% with and without tracking, respectively, at m°_w (0.014 kg/s) with $m^{\circ}_{th,L}$ (0.0084 kg/s), and the weather conditions in the current study were similar to the weather conditions in the previous study

in the case of no tracking, and were better in the case of with tracking. The $\eta_{c.overall}$ of the current study was superior to the $\eta_{c.overall}$ of the previous study, despite using m°_{wtr} higher than the current study. This proves that the cooling system of PV by using water jet system gives higher efficiency than the cooling system in the previous studies.

Table (8): Comparison of the results of current study with the results of proceeding published studies

Ref.	Search type	Operating time	Type PV /Area	Cooling system	m° (kg/s)	Tank (L)	$m^{\circ}_{L.th}$ (kg/s)	$I_{av.}$ (W/m ²)	$T_{av.amb}$ (°C)	$\eta_{c.overall}\%$
[3] Shihabud -heen and Arun 2014	Practical & theoretical	9:00am to 5:00 pm	Mono/ 2.1m ²	Absorber plate , copper tubes and glass cover	0.01	100	-	510	-	39.8 Without tracking
[9] Barone et al. 2019	Practical & theoretical	10:40am to 17:00pm	Poly/ 1.62m ²	Plastic tubes with aluminum box	0.016	60	-	810	26	38.6 With tracking
Current Work	Practical/ Thermal	8:30am to 4:30pm	Mono/ 1.006m ²	water jet	0.014	20	0.0063	789	24	48 Without tracking
Present Work	Practical/ Thermal	8:30am to 4:30pm	Mono/ 1.006m ²	water jet	0.014	20	0.0084	1015	39	52 With tracking

5. Conclusions

The electrical and thermal performance of the PVT is enhanced to the best level with the presence of cooling system and tracking, and it can be concluded that:

- 1- The PVT is more efficient than the PV.
- 2- The $\eta_{s.overall}$ and $\eta_{c.overall}$ increase with increasing $m^{\circ}_{th.L}$.
- 3- Cooling the PVT leads to an increase in the all E.P produced from it, and Q_{th} is used to heat the water.
- 4- The Q_{el} produced by the PVT increases directly with the increase of both solar radiation and $m^{\circ}_{th.L}$.
- 5- The highest total energy produced was in the presence of tracking at 0.0084 kg/s, which is (13.13 MJ).
- 6- The $\eta_{s.overall}$ with tracking is greater than the $\eta_{s.overall}$ without tracking at the same main flow rate and $m^{\circ}_{th.L}$.

References

- [1] S. K. Firth and D. Ph, "Raising Efficiency in Photovoltaic Systems : High Resolution Monitoring and Performance Analysis Systems : High Resolution Monitoring," The Institute of Energy and Sustainable Development, De Montfort University, 2006.
- [2] H. A. Hussien, A. H. Numan, and A. R. Abdulmunem, "Improving of the photovoltaic / thermal system performance using water cooling technique," *IOP Conf. Ser. Mater. Sci. Eng.*, vol. 78, no. 1, 2015, doi: Copyrights @Kalahari Journals Vol. 7 No. 1(January, 2022)

- 10.1088/1757-899X/78/1/012020.
- [3] M. Shihabudheen and P. Arun, "Performance evaluation of a hybrid photovoltaic-thermal water heating system," *Int. J. Green Energy*, vol. 11, no. 9, pp. 969–986, 2014, doi: 10.1080/15435075.2013.833931.
 - [4] H. M. S. Bahaidarah, "Experimental performance evaluation and modeling of jet impingement cooling for thermal management of photovoltaics," *Sol. Energy*, vol. 135, pp. 605–617, 2016, doi: 10.1016/j.solener.2016.06.015.
 - [5] S. S. Faiz F. Mustafa, Athmar thamer naiyf Falah I. Mustafa, "Simple design and implementation of solar tracking system two axis with four sensors for Baghdad city," *2018 9th Int. Renew. Energy Congr.*, no. Irec, pp. 1–5, 2018, doi: 10.1109/IREC.2018.8362577.
 - [6] A. El Hammoumi, S. Motahhir, A. El Ghzizal, A. Chalh, and A. Derouich, "A simple and low-cost active dual-axis solar tracker," *Energy Sci. Eng.*, vol. 6, no. 5, pp. 607–620, 2018, doi: 10.1002/ese3.236.
 - [7] H. A. Hasan, K. Sopian, and A. Fudholi, "Photovoltaic thermal solar water collector designed with a jet collision system," *Energy*, vol. 161, pp. 412–424, 2018, doi: 10.1016/j.energy.2018.07.141.
 - [8] P. Module, J. Kim, S. Bae, Y. Yu, and Y. Nam, "Experimental and Numerical Study on the Cooling Performance of Fins and Metal Mesh Attached on a Photovoltaic Module," *Energies* 2020, *13*, 85, pp. 1–12, 2019.
 - [9] G. Barone, A. Buonomano, C. Forzano, A. Palombo, and O. Panagopoulos, "Photovoltaic thermal collectors: Experimental analysis and simulation model of an innovative low-cost water-based prototype," *Energy*, vol. 179, pp. 502–516, 2019, doi: 10.1016/j.energy.2019.04.140.
 - [10] E. B. Agyekum, S. Praveenkumar, N. T. Alwan, V. I. Velkin, S. E. Shcheklein, and S. J. Yaqoob, "Experimental Investigation of the Effect of a Combination of Active and Passive Cooling Mechanism on the Thermal Characteristics and Efficiency of Solar PV Module," *Inventions* 2021, *6*, 63, pp. 1–17, 2021.
 - [11] M. A. Eleiwi, "Heat Pipe Solar Collector With Automatic Tracking System," Doctoral Thesis, Mech.Eng.Dept.Uneversity of Technology, 2016.
 - [12] M. A. Eleiwi and H. S. Shallal, "Thermal performance of solar air heater integrated with air–water heat exchanger assigned for ambient conditions in Iraq," *Int. J. Ambient Energy*, vol. 0750, 2020, doi: 10.1080/01430750.2020.1722745.
 - [13] M. F. Mohammed, M. A. Eleiwi, and K. T. Kamil, "Experimental Investigation of Thermal Performance of Improvement a Solar Air Heater With Metallic Fiber," *Energy Sources, Part A Recover. Util. Environ. Eff.*, vol. 43, no. 18, pp. 2319–2338, 2021, doi: 10.1080/15567036.2020.1833110.
 - [14] M. A. Eleiwi, A. A. M, and,F. M. Abed. Saleh "Effect of Filling Ratio and Tracking System on Performance of Wickless Heat Pipe Parabolic Trough Solar Collector with Evacuated Glass Tube", *Adv. Nat. Appl. Sci.*, vol. 9, no. November, pp. 23–31, 2015.
 - [15] S. M. Talib, F. L. Rashid, and M. A. Eleiwi, "The effect of air injection in a shell and tube heat exchanger," *J. Mech. Eng. Res. Dev.*, vol. 44, no. 5, pp. 305–317, 2021.
 - [16] N. D. Mokhlif, M. A. Eleiwi, and T. A. Yassen, "Experimental investigation of a double glazing integrated solar water heater with corrugated absorber surface," *Mater. Today Proc.*, vol. 42, pp. 2742–2748, 2021, doi: 10.1016/j.matpr.2020.12.714.
 - [17] T. A. Yassen, N. D. Mokhlif, and M. A. Eleiwi, "Performance investigation of an integrated solar water heater with corrugated absorber surface for domestic use," *Renew. Energy*, vol. 138, pp. 852–860, 2019, doi: 10.1016/j.renene.2019.01.114.
 - [18] M.A. Eleiwi, F.M. Abed, A.A.M. Saleh, "Performance investigation of a wickless heat pipe parabolic trough solar collector", *Eur. J. Sci. Res.* 136 (4) (2015) 377–394.
 - [19] F. M. Abed, M. A. Eleiwi, M. Hasanuzzaman, M. M. Islam, and K. I. Mohammed, "Design, development and effects of operational conditions on the performance of concentrated solar collector based desalination system operating in Iraq," *Sustain. Energy Technol. Assessments*, vol. 42, no. June, p. 100886, 2020, doi: 10.1016/j.seta.2020.100886.
 - [20] Muhammad Asmail Eleiwi, Mohammed Fowzi Mohammed, and K. T. K. (in press). "Eperimental Analysis of Thermal Performance of a Solar-Air Heater with a Flat Plate and Metallic Fiber," *J. Eng. Scince Technol.*

Nomenclature

A	Area of the PV module (m^2)	$T_{\text{colle.in}}$	Temperature of the working fluid inlet to collector ($^\circ\text{C}$).
Ac	Area of collector (m^2)	$T_{\text{colle.out}}$	Temperature of the working fluid outlet to collector ($^\circ\text{C}$).
CP_{wtr}	Heat capacity of the water ($\text{J/kg.}^\circ\text{C}$)	$T_{\text{pv av.}}$	Average temperature of PV panel ($^\circ\text{C}$)
I_m	Maximum current of PV (A)	$T_{w.i}$ ($^\circ\text{C}$)	Initial tank water temperature ($^\circ\text{C}$)
I_{sc}	Short-circuit current of solar cell (A)	$T_{w.f}$ ($^\circ\text{C}$)	Final tank water temperature ($^\circ\text{C}$)
V_m	Maximum voltage of PV (V)	T_{tank}	Tank water temperature ($^\circ\text{C}$)
I	Solar radiation (W/m^2)	$T_{w \max}$	Maximum tank water temperature ($^\circ\text{C}$)
Q_{in}	The total incoming solar radiation energy(MJ)	T_{amb}	Ambient temperature ($^\circ\text{C}$)
Q_{out}	Total energy output(MJ)	$T_{(PVT,PV) \max}$ ($^\circ\text{C}$)	The maximum temperature of PVT, PV panels ($^\circ\text{C}$).
Q_{stor}	Thermal energy stored in the tank(MJ)	$T_{\text{th.L.out}}$	Temperature of the hot water drawn from the HWT ($^\circ\text{C}$).
Q_L	Thermal energy of thermal load (MJ)	$T_{\text{c.w.in}}$	Temperature of the cold water supplied to the HWT ($^\circ\text{C}$).
Q_{el}	Total electrical energy of PVT,PV (MJ)	m_{wtr}°	Water mass flow rate of collector (kg/s)
Q_{th}	Total thermal energy of PVT (MJ)	$m_{\text{th.L}}^\circ$	Mass flow rate of thermal load (kg/s)
$E.P$	E.P (w)	M_{wtr}	Mass of water in the tank (kg)
$t (s)$	The time of global solar radiation during the day	T_{amb}	Ambient temperature ($^\circ\text{C}$)

Greek symbols

$\eta_{el.PV}$	Mean daily electrical efficiency of PV
$\eta_{el.PVT}$	Mean daily electrical efficiency of PVT
η_{d-th}	Mean daily thermal efficiency of system
$\eta_{overall}$	Overall efficiency
$\eta_{s.overall}$	Daily overall efficiency of system
$\eta_{c.overall}$	Daily overall efficiency of collector
ϕ	Relative humidity

Abbreviations

PVT	Hybrid photovoltaic thermal collector
PV	Reference photovoltaic collector
HWT	Hot water tank
CWT	Cold water tank
SS	Selector switch